RESEARCH ARTICLE

Design and Evaluation of Repaglinide Nanosuspension for Oral Controlled Drug Delivery System by using 3^2 Factorial Design

Sonali Vijaykumar Magdum[1*], Pramodkumar Jaykumar Shirote[2]

[1]*Department of Pharmaceutics, Dr. J. J. Magdum Pharmacy College, Jaysingpur, Kolhapur, Maharashtra-416101, India*
[2]*Department of Pharmaceutical Chemistry, Dr. Bapuji Salunkhe Institute of Pharmacy, Miraj-416410, India*

Received: 4th Jan, 2025; Revised: 13th Feb, 2025; Accepted: 21st May, 2025; Available Online: 25th Jun, 2025

ABSTRACT
The current work proposed a nanocrystal-based formulation to overcome the solubility issues of repaglinide. Using the lyophilization procedure, REP nanosuspension was successfully transformed towards solid form. To make also preserve REP nanosuspension, polyvinyl alcohol as well as Eudragit S100 were used as protectors. Lyophilization's suitability for enhancing physical stability was assessed by considering important restrictions, such as the shape of solid dispersion, on the characteristics of nanosuspension. The generated nanocrystals' solid-state characteristics were also evaluated. Process factors that were improved increased the polydispersity index, zeta potential, drug content, also average particle size. Selective cryoprotectants (lactic acid) were used to assess the lyophilization procedure as an appropriate solidification approach. With an average particle diameter of 317 ± 3.4 nm, PDI about 0.150, also zeta potential about -10.2 ± 0.85 mV, formulation remained stable throughout three months at 4°C. The generated nanosuspension's discharge profile showed a cumulative release of over 92.23%, compared to 8.02% during the first ten hours with unprocessed medicine. These findings suggest that the new formulation successfully increases Repaglinide's water solubility.
Keywords: Repaglinide, Factorial Design, Nanosuspension, Nanoprecipitation, Drug release, Stability.
How to cite this article: Sonali Vijaykumar Magdum, Pramodkumar J Shirote. Design and Evaluation of Repaglinide Nanosuspension for Oral controlled Drug Delivery System by using 3^2 Factorial Design. International Journal of Drug Delivery Technology. 2025;15(2): 416-24. doi:10.25258/ijddt.15.2.6
Source of support: Nil.
Conflict of interest: None

INTRODUCTION

The anti-diabetic compound Repaglinide (REP), which is produced from carboxyl methyl benzoic acid, has received clearance from US Food and Drug Administration (US-FDA). That selectively targets ATP-binding membrane transporters and encourages the release of insulin from β-cells. REP interacts with other intracellular channels and influences potassium gate kinetics, gene expression, enzyme activity, and calcium homeostasis. Numerous investigations have shown that REP interacts to calcium receptors in neurons in a calcium-dependent manner. In addition, the meglitinide REP is poorly absorbed, has a short half-life, binds strongly to proteins, and is not highly soluble. An insulin-tropic medication called repaglinide selectively targets neural calcium sensors in neurons, including the well-known neuromodulator downstream regulatory domain antagonist modulator (DREAM), which is involved in several physiological processes.[1,2]

Oral administration be a highly prevalent method to give medications due to its low cost, great patient conformity, also simplicity to usage. Medications enter the circulation after oral consumption and are mostly absorbed in the stomach before being distributed to other tissues. Medications remain absorbed in gastrointestinal tract (GIT), where these pass through gastrointestinal epithelium and dissolve in luminal fluids. In oral delivery, dissolution is thought to be the rate-limiting stage. Because of their low solubility and delayed disintegration in digestive fluids, poorly soluble medications provide serious biopharmaceutical problems. According to reports, before they reach the pharmaceutical stage, 70% of possible treatment candidates are rejected because of insufficient bioavailability, which is attributable to poor water solubility.[3]

Nanocrystals have a higher drug loading capacity and require less surfactants to be stable when compared to other nano-based formulations. Because of their improved stability and simplicity of manufacturing using both top-down also bottom-up methods, researchers are becoming further and more interested with creating topical formulations using nanocrystals. Nanocrystals are an essential tool for solving a number of drug-related problems. These crystalline drug clusters have particle diameters between 10 and 1000 nm and are devoid of matrices and carriers. By increasing saturation solubility and dissolution rates, nanocrystals provide greater bioavailability than microcrystals.[4] For oral, pulmonary, nasal, ophthalmic, and injectable treatments, they are easily integrated into standard dose forms. This technology's manufacturing processes and parameters have been thoroughly examined in many publications. The focus of this study is on nanocrystal-based drug formulations and applications for a range of diseases. One effective method of enhancing solubility to medications is solid dispersion. Other techniques, such micronization and salt production, can increase the water solubility of less soluble compounds,

**Author for Correspondence: svmagdum25@gmail.com*

Table 1: Parameters for preparation of Nanocrystal

Specifications	Optimum Values
Repaglinide and Eudragit RLPO ratio	1:1, 1:2, 1:3
Concentration of Surfactant	0.5%, 1%, 1.5%

although they could have drawbacks. For many drugs, reducing particle size frequently does not improve bioavailability enough or considerably. Furthermore, salt production might be difficult, especially when neutral and weak acids are present. Furthermore, salt production might be difficult, especially when neutral and weak acids are present. For poorly soluble compounds, solid dispersion, in which the medicine is present in an amorphous form, is a viable way to increase solubility and perhaps boost oral bioavailability.[5-9]

MATERIALS AND METHODS

Materials

The kind donation of repaglinide came from Dr. Reddy's Laboratories in Hyderabad. We purchased Eudragit (RLPO) from Evonik Lab in Mumbai. Sigma Aldrich Ltd., located in Mumbai, provided the lactose and polyvinyl alcohol. We bought HPLC-grade methanol from LOBA Chemicals Pvt. Ltd. For everything else, pure analytical-grade reagents were used.

Methods

Quality by Design Approach

We used a central composite design with reaction surface technique (CCD-RSM) with Design Expert software, Trial version 13.0, to improve formulation of generated batches. This approach is suitable for a methodical evaluation of the impact of different formulation components over nine experimental runs. The concentrations of nanocrystals (Y1) and cross-povidone (Y2) were chosen as independent factors in this investigation, whereas drug release (X1), particle size (X2), also zeta potential (X3) was regarded as a variable of dependence. This analysis's goal was to comprehend how these reactions change when the values of the two chosen factors change.[10]

Table 2: Batches for preparation of Repaglinide Nanocrystal

Sr.No.	Formulation Code	Drug and Polymer Ratio in mg	Concentration of Surfactant in %
1	RN-1	1:1	0.5
2	RN-2	1:1	1
3	RN-3	1:1	1.5
4	RN-4	1:2	0.5
5	RN-5	1:2	1
6	RN-6	1:2	1.5
7	RN-7	1:3	0.5
8	RN-8	1:3	1
9	RN-9	1:3	1.5

Fabrication of Repaglinide Loaded Nanosuspension

The nano-precipitation method was employed using the solvent-antisolvent technique. Solvents including methanol and acetone were screened. Various polymers and surfactants, such as Eudragit (RLPO) and PVA were evaluated both individually and in mixture as stabilizers. Processing parameters and material characteristics, such as type of stabilizing agent, medicine with emulsifier proportion, a solvent to antisolvent ratio, and rotation velocity, have been modified to achieve desired particle size along with PDI.

An Ultrasound Processor VC505 from Sonics and Composites Inc., USA, was utilized to prepare nanoprecipitation employing probe sonication in a combined method integrating sonication. The following

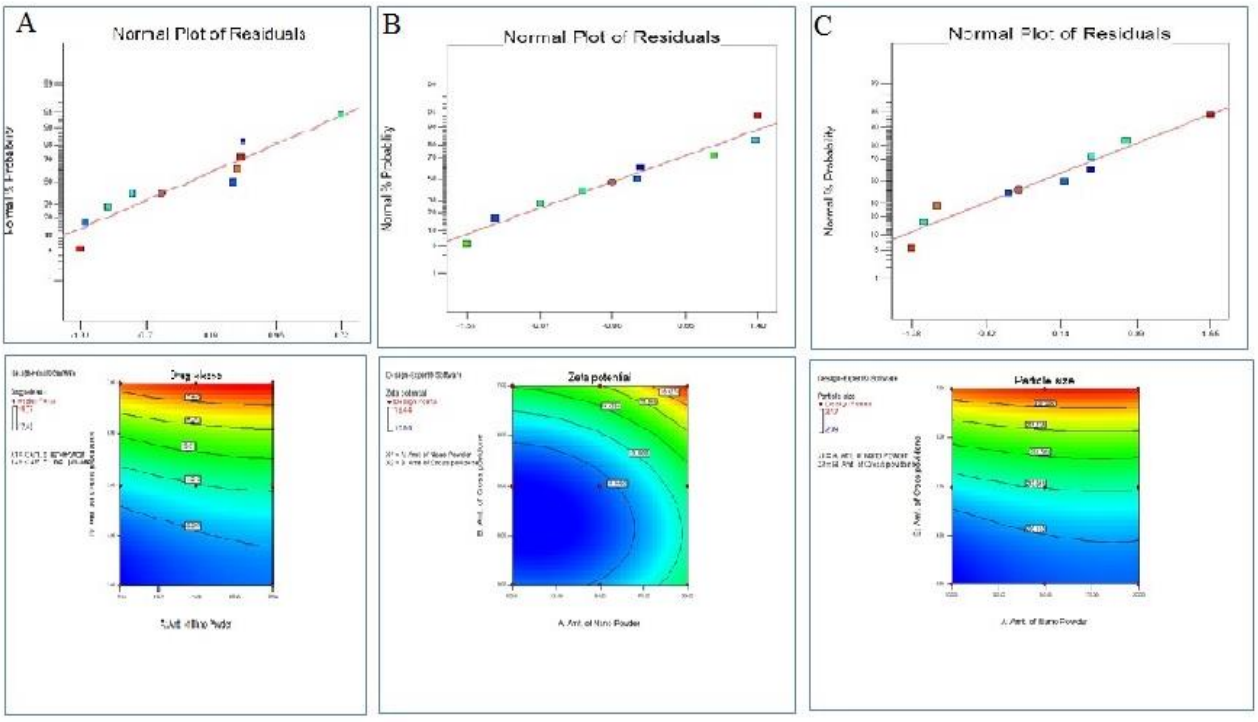

Figure 1: Counter plots and 3D responses of A) Drug release, B) Particle size, C) Zeta potential

Table 3: Physicochemical characterization of Repaglinide loaded Nanosuspension

Sr.No.	Formulation Code	Particle size (nm)	Polydispersity Index	Zeta potential (mv)	Encapsulation Efficiency
1.	RN-1	217	0.652	12.5	18.78±1.22
2.	RN-2	305	0.213	14.7	29.33±1.45
3.	RN-3	247	0.745	13.75	43.33±1.38
4.	RN-4	220	0.387	13.80	54.88±1.52
5.	RN-5	237	0.479	10.99	63.10±1.25
6.	RN-6	312	0.965	18.44	77.70±1.44
7.	RN-7	209	0.325	11.50	83.88±1.42
8.	RN-8	242	0.147	11.74	91.73±1.51
9.	RN-9	317	0.854	15.15	95.59±1.88

RN- Repaglinide loaded Nanocrystals, nm –Nanometer, mv-Millivolts
**Each value is average of three separate determinations ± SD*

Table 4: Stability study of optimized batch of nanocrystal formulation (RN9)

Months	Room Temperature (4±2 ^{0}c)		
	Particle size (nm)	Zeta potential (mv)	Entrapment efficiency (%)
0	421.2±1.25	11.3	91.91±1.37
1	417.38±2.01	11.9	90.65±1.78
2	428.77±1.65	11.1	90.23±1.22
3	422.5±2.12	11.3	90.55±2.78

processing conditions were used during the five minutes of sonication: three seconds to turn off and five seconds of 25% magnitude stimulus on. The combined process, which used HPH (High Pressure Homogenization) to form a suspension, employed a similar nanoprecipitation technique. The suspension was then examined by HPH using a Panda PLUS 1000 from GEA NiroSoavi, USA. The homogenization process was run five times at 500 bar of pressure, followed by fifteen cycles at 800 bar. Three duplicates of each run were made on the same day and three days later (n=3).[11]

Formation of Nanosuspension Solidification

A Christ alpha 4d plus lyophilizer from the USA was used to lyophilize an optimum batch to maintain the stability of the nanosuspension. Several substances were examined for possible application as cryogenic protection, including mannitol, sugar, milk sugar, sucrose, the amino acid L-D-sorbitol, HPβCD, as well as PVP-K30. Each freezing agent was added at a 10% concentration for the initial test. The nanosuspension stayed frozen at -80°C over 48 hours and then thawed within ambient temperature. There were both freezing and thawing cycles. Following thawing, measurements are made of the particle size as well as PDI. Specimens were frozen at approximately -45°C for lyophilization, and then they went through both the main and secondary drying processes. After freezing, 250 mT of variable-length main evaporation started around -30°C under vacuum (with brief pauses at -25°C).[12]

Evaluation of Repaglinide-loaded Nanosuspension using the Following Criteria

Drug Content Determination

The drug's analysis technique stayed advanced by the UV-VIS spectrophotometer (UV 1900, Shimadzu, Japan) in a phosphate buffer solution (PBS) with a pH of 7.4. One milliliter of methanol was mixed with 10 milligrams of medication to create a starting solution (100 µg/ml). Using PBS pH 7.4, the capacity was then reduced to 100 ml in the volumetric flask. Following proper neutralization of the initial solution, concentrations ranging from 2-24 µg/ml were attained. Toward ascertain λmax measurements and create a standard curve, they were subsequently scanned at 200 and 400 nm. For every reading, three copies were made (n = 3). Five milligrams of the frozen material were mixed with one milliliter Milli-Q water, also resultant sample remained then subjected to previously described analytical procedure to determine the drug concentrations. All samples were run through a 0.2 µm sieve before assessment.[13]

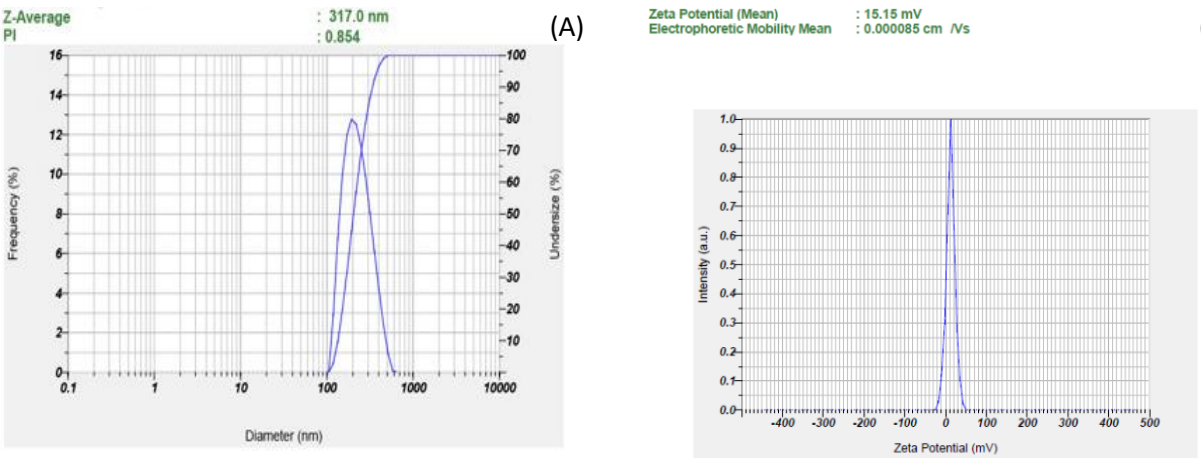

Figure 2: Analysis Report of Nanosuspension A) Particle Size B) Zeta Potential (Batch No.RN-9)

Particle Size and Zeta Potential

Depends upon idea of dynamic light diffracting, Zetasizer (HORIBA) has been utilized to determine regular particle size also the Polydispersity Index (PDI). Zeta potential has also evaluated using the same apparatus.[14] To guarantee a consistent dispersion of the sample for testing, 1 mg of frozen product has been disposed of with 3 ml by Milli-Q water also vortexed when necessary. Three copies of each measurement were made (n=3).

Determination of Encapsulation Efficiency

Three hours at 10,000 rpm and 7°C were spent centrifuging the formulation using a refrigeration centrifuge (24BL model, Remi, Mumbai, India). UV/Visible spectrophotometer (Shimadzu 1800, Japan) has been utilized determine absorbance by free drug concentration over 241nm following the supernatant's separation. The entrapment effectiveness of repaglinide was calculated from withdrawing amount of free medication with initial quantity from medication administered. Entrapment efficiency (%EE) for each formulation was calculated with the help of the following formula:

$$Entrapment\ Efficiency\ (EE\%) = ((Initial\ Drug - Final\ drug))/(Initial\ Drug) \times 100$$

Analytical Characterization

FTIR Study

With the aid of a BRUKER Alpha II FTIR Spectrophotometer, FTIR spectra were acquired for a variety of materials, including the pure API, excipients, physical mixture, and the improved formulation. After each sample, weighing around 5 mg, was examined, its spectra were collected between 400 and 4000 cm^{-1}.[15]

DSC Study

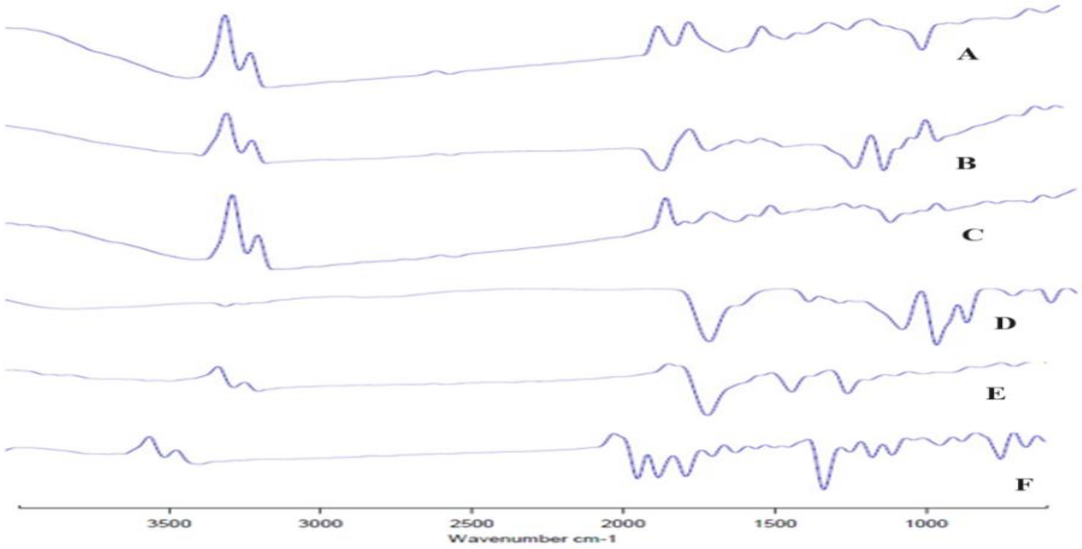

Figure 3: FTIR layout of A) Repaglinide, B) PVP K30 C) Lactic Acid D) Eudragit RS 100 E) Physical mixture (Repaglinide + PVP K30+ Lactic Acid + Eudragit RS 100), F) Formulation) (RN9)

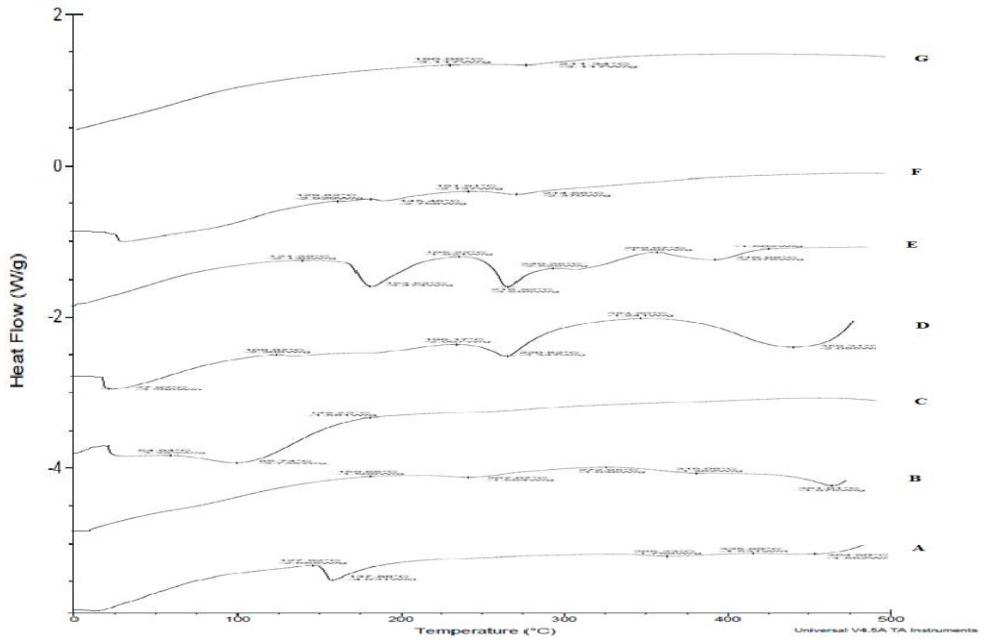

Figure 4: DSC layout for A) Repaglinide, B) PVP K30 C) Lactic Acid D) Eudragit RS 100 E) Physical mixture (Repaglinide + PVP K30+ Lactic Acid + Eudragit RS 100) F) Formulation (RN-9)

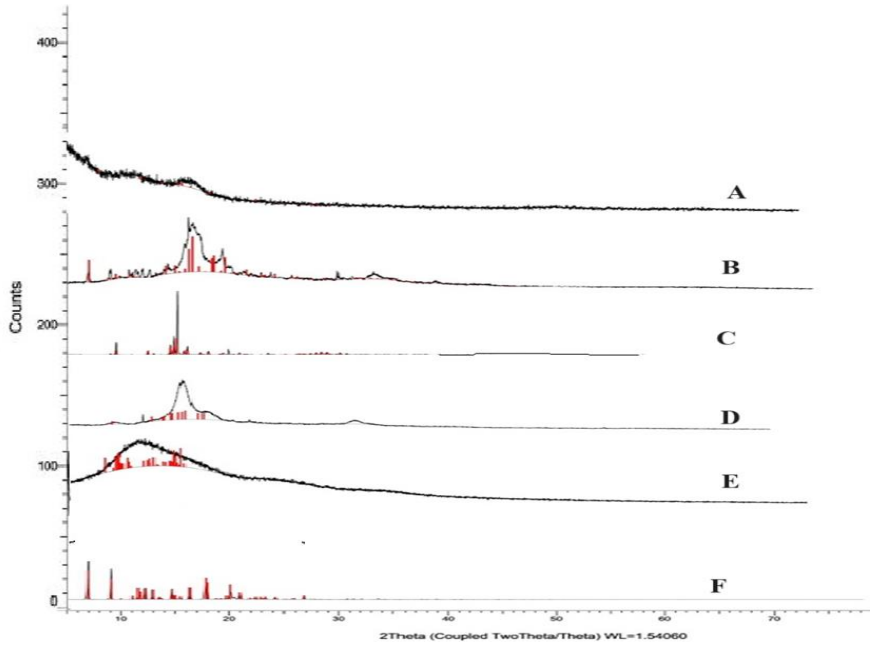

Figure 5: XRD layout of A) Repaglinide, B) PVP K30 C) Lactic Acid D) Eudragit RS 100 E) Physical mixture (Repaglinide + PVP K30+ Lactic Acid + Eudragit RS 100), F) Formulation (RN-9)

Differential Scanning Calorimetry (DSC) analysis has been implemented upon the revised formulation, physical mixtures, excipients, as well as pure medicines using a Shimadzu DSC-50 instrument, which is headquartered in Kyoto, Japan. Standard aluminum crucible pans were used to properly weigh out each sample to a capacity of 40 milliliters. After that, small holes were used to seal the lids. Samples has been warmed among 0°C too 400°C at a rate on 50°C per minute from that range. For the analysis, a nitrogen atmosphere was employed, at flow speed by 40 milliliters per minute. The crucibles were prepared for the examination by placing them on harden platform using double-sided adhesive tape.[16]

XRD Study

X-ray diffraction (XRD) has been utilized examine specimen's physical state. An XRD analyzer (Xpert MPD, Philips, Holland) was used to produce XRD images of the dried nanosuspension, lyophilized drug without the cryoprotectant, and pure drug using Cu/Ni rays. Diffractograms were scanned at a rate of 2°/min between 0° and 50° 2θ. The material was crushed with a crusher and pestle before being placed in sample containers for examination.[17]

SEM Study of Optimized Formulation

Using an atomic force microscope (Nova Scan, USA) and scanning electron microscope (Nova SEM 450, USA) in regular air, particle morphology of the lyophilized product was investigated. The scan sizes ranged from 100 nm to 800 nm, and the scan rate has been selected to 0.5 Hz. The specimen was prepared by diluting it 1:100 (1 mg in 100 ml) by double-distilled water, gently falling it on top of a glass slide, and then allowing it to dry naturally in order to prevent particle motion.[18] Data were shown using both topographic and phase imaging. For SEM research, the device worked under excitation power with 25 kV. Prior to inspection, powder specimens remained attached to metal point with adhesive two-sided tape.

In Vitro Drug Release Study

Dialysis bag's diffusion method has been utilized to examine drug absorption by raw as well as powdered form in vitro. Each dialysis bag was made and sealed securely using frozen powder and raw medication (i.e., dose equivalent; 2 mg). These bags were then immersed in 250 cc of saline with phosphate buffered (pH 7.4) to maintain sink conditions. Temperature for organization has been kept over 37 ± 0.5 °C with constant electromagnetic stirring at a speed of 100 rpm/min. At predetermined intervals, 5 milliliters of material were removed via receptor compartment then changed through fresh intermediate. 48-hour discharge research was carried out. UV spectrophotometry at 241 nm was used to measure quantity of medication dissolved, adhering to previously defined procedure.[19]

Estimation of Drug Release Kinetics

Drug's discharge dynamics from the nanocrystal composition were thoroughly investigated using a variety of kinetic equations, namely zero-order release kinetics, first-order release kinetics, and Higuchi model. Our analysis of release statistics produced a number of important indicators. Release rate constant ('n') and the time element ('k'), respectively, were specified. In addition, we computed regression coefficient, or "R," using the Korsemeyer-Peppas equation, which provided crucial information on the release procedure. We match observed dissolution data with several kinetic models in order to decipher fundamental mechanism of drug release. These models included Higuchi, Hixson-Crowell, zero-order, first-order, and Korsemeyer-Peppas versions. With use of this thorough process, we were able to evaluate regression values' (R^2) goodness of fit and choose model that best explained release behaviour.[20]

Stability Studies

Formulation was kept at 4°C to begin stability tests for nanosuspension, and samples were taken on days 1, 7, 15,

30, 60, and 90. All removed samples' size and PDI values were made using Zetasizer (HORIBA) in accordance with same procedure as previously outlined in sections. Three (n=3) duplicates of each study were carried out.[21]

RESULTS AND DISCUSSION

Data Optimization of 3^2 Full Factorial Design

Quadratic Equations

Quadratic equation for the response as follow:

$Y = \beta0 + \beta1\ A + \beta2\ B + \beta3\ AB + \beta4\ A2 + \beta5\ B2$

n these equations, Y variable that independent. Computed coefficient for factor A is represented by the value 1, whereas the average response from nine experimental runs is shown by the value 0. The average result when each element is separately changed between its lower and greater values is shown by the primary effects of factors A and B. Conversely, when both factors are varied simultaneously, the result varies as indicated by the relational terms (AB).[22,23]

The chosen independent parameters have a considerable impact on drug release, particle size (PDI), & zeta potential (ZP), as demonstrated by a thorough examination through the Design of Experiments data.The polynomial equations provided serve as a tool for drawing conclusions based on the mathematical signs within them. A positive sign suggests a synergistic impact, where factors work together, while a negative sign indicates an antagonistic effect, where factors counteract each other.

$Y1 – (\%\ DR) = 91.23 - 0.21\ A - 0.66B - 0.20\ AB - 2.597\ A^2 + 2.48\ B^2$

$Y2 – (ZP) = 11.65 + 1.47\ A + 1.75\ B - 0.36\ AB - 0.75\ A^2 - 2.20B^2$

$Y3 – (PS) = 244.47 + 4.67\ A + 2.47\ B - 1.00\ AB - 0.3.67A^2 + 21.33\ B^2$

Where, A = Amount of Nanosuspension powder

B = Amount of cross povidone

Statistical Analysis

Design-Expert Software (version 11.0) was used to do a study of variance, or ANOVA, with the aim to determine which factors were not significant. The findings demonstrated statistically significant outcomes for all from dependent variables, with p-values less than 0.05 ($p < 0.05$). The regression model is essential, as evidenced by the predicted F values for the %EE, PS, & ZP, which are 91.23, 11.65, and 244.47, accordingly.

Counterplots with Three-Dimensional Responses Showing the Impact of Different Nanocrystal Amounts and Cross-Povidone

Three-dimensional in nature plots have been developed based on the observed response in order to quantify the response's region modification. Increased drug release through the created powder as a result of raising the quantity of the nanosuspension particles as well as super disintegrant, according to an analysis of the counter plots & 3D responses for A)% Drug release, B) Particle size, and C) Zeta potential.(Fig.1 A, Fig.1 B also Fig.1 C).

Particle Size, Poly-dispersity Index and Zeta Potential

The prepared batches' particle dimensions range from 217 nm 317 nm. Minimum drug polymer ratio with minimum concentration of surfactant produce smaller particle size like RN-1, RN-4 and RN-7 was 217nm ,220nm and 209nm respectively. Moreover drug polymer ratio 1:2 with surfactant 1% produced larger particle size such as RN-2,RN-5 and RN-8 was 305nm,237nm and 242nm respectively. Some of the exceptionally result was obtained like RN-3 it should be higher particle size as compared to RN-2. Zeta potential is an essential part that impacts how potential stability and surface charge are determined in nanoparticulate systems. Greater zeta potential magnitudes, whether positively or negatively charged, often contribute to prolonged stability due to the electrostatic dislike among particles of like charges, which impedes combination. Overall result for particle size, Zeta Potential, Polydispersity Index as well as entrapment efficiency RN-9 is the optimized batch which is taken for further solid dispersion process.

Determination of Encapsulation Efficiency

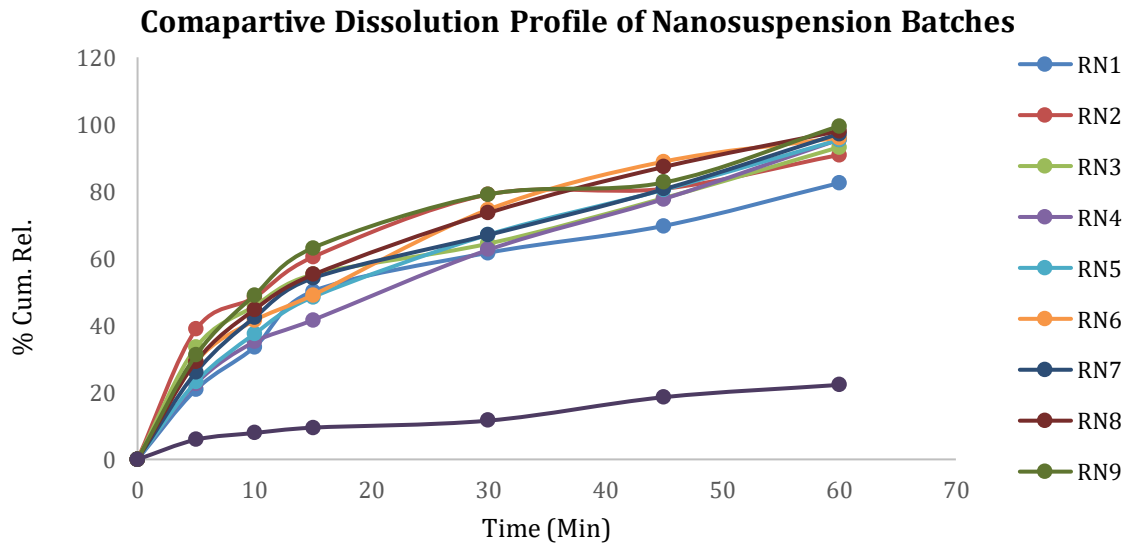

Figure 6: Comparative Dissolution Profile

Table 3 illustrates that with a larger ratio of polymer to drug, the drug encapsulation efficiency rise from 18.78±1.22% to 95.59±1.88%.

Compatibility Study by FTIR

The observed spectra showed that -OH stretching was responsible for the prominent (sharp) peak at 760.67cm^{-1}. The prominent peak observed at 1210.47 cm^{-1} is attributed to several stretching vibrations, including C-N stretching (triazole), N-H stretching (amino), N=N=N stretching (amine), and C-Cl stretching. Corresponding peaks at 2888.67 cm^{-1}, 1561.94 cm^{-1}, and 760.67 cm^{-1} also arise from these stretching modes. Additionally, the strong peak at 1631.36 cm^{-1} is indicative of existence for triazole ring and C=O extending (ketone) vibrations. Features of PVP K30's spectra PVP K30 has been shown to have three distinct peaks: an O-H stretching peak around 3063.59 cm-1, a C-H aliphatic extending peak at 2893.23 cm-1 as well as 2828.13 cm-1, plus an aromatic C=O extending peak about 1644.90 cm-1. Characteristic peak for lactic acid's spectrum, noticed at 3396.71 cm-1, was brought about by O-H stretching; additional peaks, in 2990.42 cm-1, were caused by C-H stretches vibrations; C-H bending vibrations were present at 1456.63 cm-1 too 1210.63 cm-1; along with C-O extending movements on esters were responsible for peaks, at 1121.26 cm-1 or 1040.71 cm-1. Intensity 743.43 cm-1 indicates an aromatic substitution-attributed. The signature spike of Eudragit S100, which can be seen at 3022.52 cm-1, is caused by O-H axial distortion. Another reach their highest point, at 1557.75 cm-1, is produced via C=O extending movements. Peak, over 981.75 cm-1, has been caused by existence on C-O sections that contain enol linkages.

The actual mixture's spectrum shows distinctive peaks. O-H axial distortion is found at 2916.18 cm^{-1}; C=O stretching (ketone) is associated with it at 1693.11 cm^{-1}; N=N=N stretching (amine) is linked to it at 1507.95 cm^{-1}; C-H bending vibrations are responsible over it during 1452.24 cm^{-1}; C-N stretching (triazole) is connected to it during 1219.27 cm^{-1}; -OH stretches is found at 821.84 cm^{-1}; as well as C-Cl stretching—which additionally suggests aromatic in nature substitution—is accountable at 731.28 cm^{-1}. There are currently no drug-polymer contradictions, according to an FTIR study of the actual mixture.

Differential Scanning Calorimetry

The technique of Differential Scanning Calorimetry was used to examine material's melting & the recrystallization characteristics. Repaglinide, RLPO, PVP K-30, PVA, a physical mixture containing lactic acid, and the formulation RN-9 were among the compounds whose thermograms obtained from the DSC were studied .

Repaglinide's crystalline structure is shown by a notable endothermic value at 138°C on the DSC thermogram. RLPO shows a distinct melting endotherm at around 268.85°C. PVP K-30 exhibits notable melting endotherms at 137.95°C and 101.93°C. The thermal curve for PVA displays a prominent melting point endotherm at 224.98°C. The physical mixture's thermal curve presents sharp melting point endotherms at 137.02°C, 138.32°C, and 224.89°C. The formulation RN-9 shows a peak at 137.91°C

XRD Study

The drug's crystal structure was confirmed by X-ray diffraction (XRD) evaluation, which revealed typical maxima at 2θ values of 18.76, 19.55, 21.11, 23.4, and 25.08. As seen in Fig. 5, the magnitude of those peaks dramatically decreased after lyophilization, suggesting that the substance had substantially amorphized within the frozen sample. Many researches have proven this partial amorphization of the active component during lyophilization process.[24]

This change is most likely the result of the demanding freeze-drying procedure, which causes water to crystallize and then sublimate. Amorphization results from changes in structure that those certain solutes experience throughout the chilling process, which turns the solution into a solid state.

In Vitro Dissolution Study

In vitro medication release study suggests that over 60 min. period, the profile of release of the raw medication showed just a slight increase in the amount released. In contrast, throughout the same period, the manufacturing process demonstrated a steady and progressive rise in the release of drugs. According to the in vitro research, using this technique produced repaglinide which was distributed more evenly.

Drug Release Kinetics Study

The R^2 values as well as regression coefficients that were obtained by matching empirical *in vitro* dissolution findings with log incremental proportion for medication release against log time Korsmeyer-Peppas equation. All the repaglinide nanocrystal based solid dispersion *in vitro* release dynamics were investigated by the researchers. The regression coefficients (R2) for every batch of nanosuspension across several kinetics' parameters are also included in the following table. According to the study of the kinetic statistics, Korsmeyer-Peppas (K-P) model offered more effective fit of explaining in vitro dissolution through nanocrystals. The diffusional release coefficient 'n,' ascertained from the proposed model's slopes, varied between 0.658 and 0.863. The fact that these ratios are between 0.41 and 0.80 indicates all of the formulations appear to have Fickian release mechanisms.

Stability Studies

Over the course of three months, the drug nanosuspension showed just a minor enlargement in size while remaining robust at 4°C. Sampling at various intervals indicated minimal increases in both size. Instabilities in nanosuspensions are often caused by Ostwald ripening, a procedure whereby bigger the crystallites proliferate at the costs of tiny ones. Particle dimensions increases are commonly used to characterize this phenomenon. These increases cause nanocrystals to expand into the micron range and cause sample homogeneity to be lost, which suggests physical instability. However, the nanosystem in this study showed physical stability under storage conditions, with only slight increases in size and PDI.

CONCLUSION

An intact nanosuspension dosage form for the drug Repaglinide was successfully developed using a straightforward nano-precipitation approach that used RLPO with PVP K-30 as surfactants. This nanosuspension's

average particle size, PDI, as well as zeta potential were 317 nm, 0.658, also 1.98 mV, correspondingly. Stability tests at 4°C showed no size growth, demonstrating the formulation's exceptional resilience under these conditions. As a solidification method, lyophilization was used with cryoprotectants such lactic acid. Compared to the ~21% release seen with the unprocessed medication; *in vitro* release experiments showed an astounding ~88% drug release during the first 10 hours. It suggests that the new formulation effectively increases the reported solubility of the drug Repaglinide through the application of nanonization technology.

Acknowledgement
Authors are grateful to Govt. College of Pharmacy, Karad, Satara, MS, India for offering excellent research infrastructure throughout completion for present investigation

REFERENCES

1. Ma Y, Yang Y, Xie J, Xu J, Yue P, Yang M. Novel nanocrystal-based solid dispersion with high drug loading, enhanced dissolution, and bioavailability of andrographolide. Int J Nanomedicine. 2018; 13:3763-3779. https://doi.org/10.2147/IJN.S164228.
2. Jermain SV, Brough C, Williams III RO. Amorphous solid dispersions and nanocrystal technologies for poorly water-soluble drug delivery–an update. Int J Pharm. 2018; 535:379-392. https:// doi.org/ 10.1016/j.ijpharm.2017.10.051
3. Jakubowska E, Lulek J. The application of freeze-drying as a production method of drug nanocrystals and solid dispersions–a review. J Drug Deliv Sci Technol.2021;62:102357. https://doi.org/10.1016/j.jddst.2021.102357
4. Ding Z, Wang L, Xing Y, Zhao Y, Wang Z, Han J. Enhanced oral bioavailability of celecoxib nanocrystalline solid dispersion based on wet media milling technique: formulation, optimization and *in vitro/in vivo* evaluation. Pharmaceutics.2019;11:328-345.https://doi.org/ 10.3390/pharmaceutics11070328.
5. Kaur A, Parmar PK, Bansal AK. Evaluation of different techniques for size determination of drug nanocrystals: A case study of celecoxib nanocrystalline solid dispersion. Pharmaceutics. 2019; 11:516-533. https:// doi.org/10.3390/pharmaceutics11100516.
6. Rahman M, Arevalo F, Coelho A, Bilgili E. Hybrid nanocrystal–amorphous solid dispersions (HyNASDs) as alternative to ASDs for enhanced release of BCS Class II drugs. Eur J Pharm Biopharm. 2019;145:12-26. https:// doi.org/10.1016/j.ejpb.2019.10.002.
7. Ahuja M, Dhake AS, Sharma SK, Majumdar DK. Diclofenac-loaded Eudragit S100 nanosuspension for ophthalmic delivery. *J Microencapsul*. 2011;28(1):37–45. doi:10.3109/02652048.2010.523794
8. Schaffazick SR, Pohlmann AR, Dalla-Costa T, Guterres S.l.S. Freeze-drying polymeric colloidal suspensions: Nanocapsules, nanospheres and nanodispersion. A comparative study. *Eur J Pharm Biopharm*. 2003;56:501–505. doi:10.1016/S0939-6411(03)00139-5
9. Abdelwahed W, Degobert G , Serge Stainmesse S, et al. Freeze-drying of nanoparticles: Formulation, process and storage considerations. *Adv Drug Deliv Rev*. 2006;58(15):1688-1713. doi:10.1016/j.addr.2006.09.017
10. Pignatello R, Ricupero N, Bucolo C, Maugeri F, Maltese A, Puglisi G. Preparation and characterization of eudragit retard nanosuspensions for the ocular delivery of cloricromene. AAPS PharmSciTech **2006;** 7: E192–E198
11. Das S, Suresh P, Deshmukh R. Design of eudragit RL 100 nanoparticles by nanoprecipitation method for ocular drug delivery. *Nanomed Nanotech Bio Medi* **2010**; *6:* 318-323.
12. S. Motwani, S. Chopra, S. Talegaonkar , K. Kohli, F.Ahmad, R. Khar, Chitosan-sodium alginate nanoparticles as submicroscopic reservoirs for ocular delivery: formulation, optimization and *in vitro* characterization, Eur J Pharm Biopharm 68 (2008) 513–525
13. Castelli F, Messina C, Sarpietro M, Pignatello R, Puglisi G. Flurbiprofen release from Eudragit RS and RL aqueous nanosuspension: a kinetic study by DSC and dialysis Experiments. *AAPS PharmSciTech* **2002**; 3: E9.
14. C. Hong, Y. Dang, G. Lin, Y. Yao, Effects of stabilizing agents on the development of myricetin nanosuspension and its characterization: An in vitro and in vivo evaluation, Int. J of Pharm. 477 (2014) 251–260.
15. Bilati U, Allémann E, Doelker E. Nanoprecipitation versus emulsion-based techniques for the encapsulation of proteins into biodegradable nanoparticles and process-related stability issues. *Aaps Pharmscitech*. 2005;6(4):E594–E604. doi:10.1208/pt060474
16. Adibkia K, Omidi Y, Siahi M. Inhibition of Endotoxin-Induced uveitis by methylprednisolone acetate nanosuspension in rabbits. *J Ocul Pharmacol Ther* 2007*;* 23: 421-432.
17. Tran P, Pyo YC, Kim DH, Lee SE, Kim JK, Park JS. Overview of the Manufacturing Methods of Solid Dispersion Technology for Improving the Solubility of Poorly Water-Soluble Drugs and Application to Anticancer Drugs. Pharmaceutics.2019;11:132.https://doi.org/10.3390/pharmaceutics11030132.
18. Sarnes A, Kovalainen M, Häkkinen MR, Laaksonen T, Laru J, Kiesvaara J, Ilkka J, Oksala O, Rönkkö S, Järvinen K, Hirvonen J. Nanocrystal-based per-oral itraconazole delivery: Superior *in vitro* dissolution enhancement versus Sporanox® is not realized in *in vivo* drug absorption. Control Release. 2014;180:109-116. https://doi.org/ 10.1016/j.jconrel.2014.02.016.
19. Hezha A A, Hunar K O, Solubility Enhancement of a Poorly Water-Soluble Drug Using Hydrotropy and Mixed Hydrotropy-Based Solid Dispersion Techniques. Hindawi Advances in Pharmacological and Pharmaceutical Sciences. 2022; 1-16. https://doi.org/10.1155/2022/7161660.

20. Pandi P, Bulusu R, Kommineni N, Khan W, Singh M. Amorphous solid dispersions: An update for preparation, characterization, mechanism on bioavailability, stability, regulatory considerations, and marketed products. Int J Pharm. 2020; 586:119560-119582. https://doi.org/10.1016/j.ijpharm.2020.119560.
21. Nkansah P, Antipas A, Lu Y, Varma M, Rotter C, Rago B, El-Kattan A, Taylor G, Rubio M, Litchfield J.J. Development and evaluation of novel solid nanodispersion system for oral delivery of poorly water-soluble drugs. J. Control.Rel. 2013;169:150-161. doi: 10.1016/j.jconrel.2013.03.032.
22. Dash S, S.Murthy, P.Chowdhury, Kinetic modeling on drug release from controlled drug delivery systems, Acta Pol Pharm 2010; 67(3): 217-223.
23. Palanisamy M, Khanam J. Solid dispersion of prednisolone: solid state characterization and improvement of dissolution profile. Drug Dev Ind Pharm. 2011;37:373-386.
24. Wang Y, Wang W, Yu E, Zhuang W, Sun X, Wang H, Li Q. Preparation of a camptothecin analog FLQY2 self-micelle solid dispersion with improved solubility and bioavailability. J Nanobiotechnology.2022;20:402. doi: 10.1186/s12951-022-01596-2.